Testing a New Multipass Laser Architecture on Beamlet

C. S. Vann S. Seznec
F. Laniesse J. E. Murray
H. G. Patton B. M. Van Wonterghem

Introduction

We completed proof-of-principle tests on Beamlet for a new multipass laser architecture that is the baseline design for the French Megajoule laser and a backup concept for the U.S. National Ignition Facility (NIF) laser. These proposed laser facilities for Inertial Confinement Fusion (ICF) research are described in their respective *Conceptual Design Reports*.[1,2] The lasers are designed to deliver 1.8 MJ and 500 TW of 0.35-μm light onto a fusion target using 240 independent beams for the Megajoule laser and 192 beams for the NIF laser. Both lasers use flash-lamp pumped glass amplifiers and have approximately 38-cm square output beams. However, there are significant differences in their architecture.

Figure 1 shows the NIF baseline architecture. A single beam consists of three amplifier modules with a total of 19 laser slabs, cavity and transport spatial filters, two cavity mirrors to form a multipass cavity, and a full-aperture Pockels cell and polarizer to switch the beam out of the cavity after four passes. During a shot, a beam from the optical pulse generator is injected into the transport spatial filter. The beam passes through the booster amplifier, makes four passes through the cavity amplifier, exits the cavity, and again passes through the booster amplifier and out of the laser towards the target. The Pockels cell and polarizer are required to switch the beam out of the cavity. After pass 1, the Pockels cell is turned "on" to rotate the beam polarization 90°, making passes 2 and 3 the correct polarization to pass through the polarizer and stay in the cavity. The Pockels cell is turned "off" at the end of pass 3, so pass 4 reflects off the polarizer to leave the cavity. Because the beam is reflected out of the cavity, the booster amplifier is at a different level than the cavity amplifier.

In contrast, the Megajoule laser and the NIF backup designs do not use a full-aperture Pockels cell and polarizer to switch the beam out of the cavity. Instead, they use a relatively small set of optics, called a Reverser, located in the center section of the transport spatial filter to steer the beam from pass 2 to pass 3 (Fig. 2). This steering is possible because the beam is intentionally pointed off-axis through the amplifiers for both architectures so that each pass focuses at a separate location at the center of the spatial filter. (Beams are focused through a small hole at the center

FIGURE 1. A single beam of the proposed National Ignition Facility (NIF) laser. (70-50-0495-1005pb01)

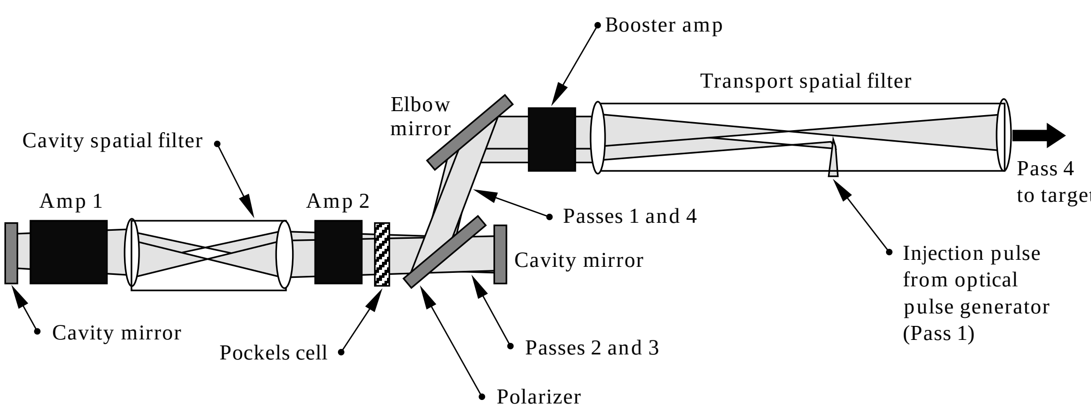

of the spatial filter to remove high spatial-frequency noise from the beam.) Separation of the passes permits the Reverser to extract the beam on pass 2, manipulate it, and re-inject it on pass 3. This same feature permits beam injection into the laser using a small mirror near the pinholes as shown in Figs. 1 and 2. The energy of the beam after pass 2 is low enough that a mirror only a few centimeters square can survive without being damaged. Consequently, the beam can be turned around with small optics rather than a large Pockels cell and polarizer.

The Reverser

In its simplest form, the Reverser consists of a small pick-off mirror that directs the pass 2 beam to a collimating lens and a retro-mirror. The retro-mirror points the beam back through the same collimating lens and along the beamline of pass 3. Practical considerations lead to at least one additional turning mirror between the pick-off mirror and lens, as shown in Fig. 2, and an isolation unit to protect against back reflections. The size of the beam in the collimated section is determined by the desired fluence on the Reverser component with the lowest damage threshold. The pick-off mirrors are sized to withstand the amount of energy expected at the end of pass 2. The size of the pick-off mirrors determines the pinhole spacing, and the pinhole spacing determines the off-axis angle of the beam through the laser. This angle causes the beam position to shift slightly in the amplifier aperture from pass to pass and reduces the maximum beam size that can pass through a given amplifier aperture. Since a smaller beam size means less energy on target, this loss, called vignetting loss, should be minimized. For NIF, a pick-off mirror about 5×5 cm^2 is large enough to avoid damage, but small enough to cause about the same vignetting loss as the NIF baseline.

The French and U.S. Reverser designs are the same in principle, but are implemented differently—the French version is the L-turn and the U.S. version is the U-turn. The L-turn is simpler, with only seven components required (see Fig. 3). After the pick-off mirror, a second mirror directs the beam through a collimating lens to the cavity mirror, which is oriented to reflect pass 2 back along pass 3. The isolation system, a Pockels cell between crossed polarizers, blocks forward and backward transmission, except during a 50-ns window to allow passage of the shot pulse. The insertable half-wave plate is used for alignment, but not for a shot. Both passes 2 and 3 go through each of the L-turn components. This requires component apertures slightly larger than for the beam by itself, due to vignetting. Also, if the pulse length is long enough to overlap in time on an L-turn optic, interference increases the fluence on that optic substantially.

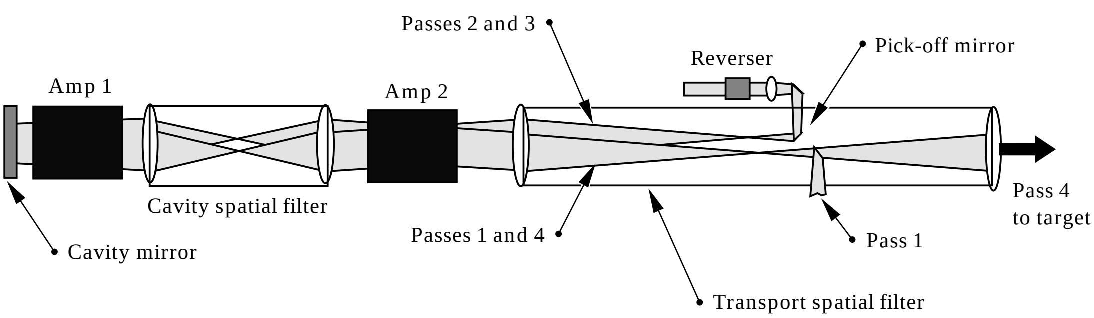

FIGURE 2. The generic Reverser in a four-pass laser architecture. (70-50-0495-1006pb01)

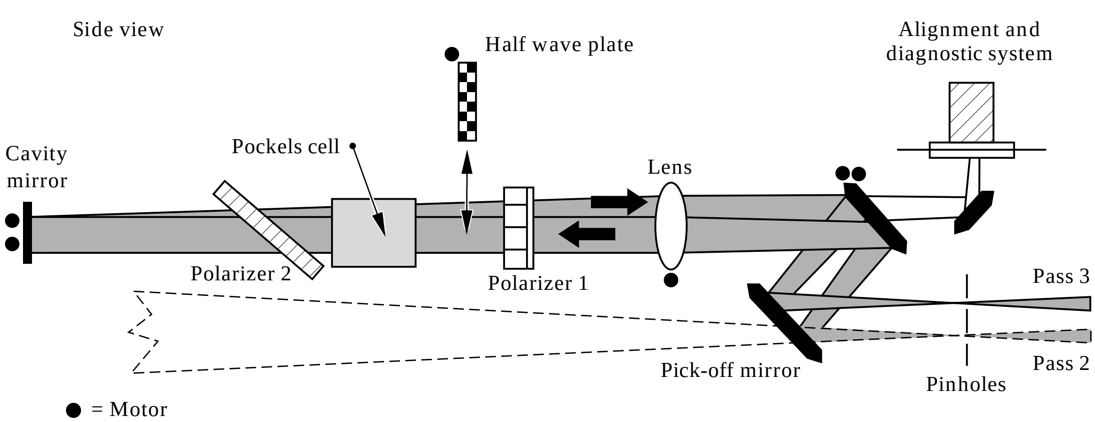

FIGURE 3. The French version of the Reverser, called L-turn. (70-50-0495-1003pb01)

In the U-turn, the pulse passes through each component only once, as shown in Fig. 4. Consequently, it has about twice as many components (13 vs 7), which are slightly smaller because there is no vignetting. The isolation system uses a half-wave plate to properly orient the polarization of the output pulse. With these exceptions, the corresponding components function the same as in the L-turn. The added complexity required to separate passes 2 and 3 in the U-turn provides design flexibility. For example, the cavity mirror of the L-turn can be replaced by a corner cube as shown in Fig. 4, which potentially improves the output pointing stability of the laser. The corner cube inverts the beam profile horizontally and vertically, so that any odd-order aberration that accumulates on passes 1 and 2, such as a drift in pointing, is canceled on passes 3 and 4.

Separation of passes 2 and 3 also makes it possible to change the beam size between passes 2 and 3. If passes 1 and 2 have a beam area about half that of passes 3 and 4, vignetting loss is determined by passes 3 and 4 only, not all four passes, which reduces vignetting loss by about 50%. This scheme also reduces aberrations, because the first two passes are through the center of the amplifiers, avoiding the more aberrated edges of the amplifier slabs. However, this scheme requires a change to the pinhole configuration that we did not attempt in these tests.

The L- and U-turn Reverser architectures have potential advantages over the NIF baseline architecture. They replace the large Pockels cell and polarizer with much smaller ones (10×10 vs 40×40 cm^2 apertures). Smaller components are lower in cost, easier to fabricate, and generally have better quality. They allow a straight, more compact layout with all the amplifier slabs in two modules to improve amplifier efficiency by reducing end losses. They eliminate the elbow mirror and one of the full-aperture cavity mirrors and allow the beam to pass through all the amplifier slabs four times. The beam passes through the booster amplifier only twice in the NIF baseline. This increases the total system amplification and allows a smaller output energy from the front end. Nevertheless, a full-size, proof-of-concept device had never been built before and was needed to establish the viability of the Reverser concept.

Joint French/U. S. Testing of the L- and U-Turn Designs

In March 1994, a team from Lawrence Livermore National Laboratory (LLNL) visited the French Centre d'Études de Limeil–Valenton (CEL-V) to discuss a joint venture to build and test a Reverser on LLNL's Beamlet laser. CEL-V had previously expressed its desire to test the L-turn on Beamlet, and U-turn tests were scheduled for early FY 1995. It was impractical to test each design independently, because of the limited time available on Beamlet (October–December 1994). Therefore, both teams hoped to jointly decide on one design.

The goal was to prove the feasibility of the basic concept. In both cases the device would be installed into the transport spatial filter of Beamlet. The requirements for isolation components and alignment and diagnostic sensors were the same. However, it was important to test the unique features of each design. Therefore, rather than decide on either the L- or U-turn, the teams jointly agreed to share responsibility for building a Reverser that could be reconfigured to test both designs by changing only a few components. The objectives were to (1) compare performance of L-turn, U-turn, and baseline concepts; (2) evaluate L- and U-turn alignment; (3) learn about control of parasitic beams caused by back reflections and amplified spontaneous emission; and (4) determine vulnerability of Reverser optics to pinhole debris.

FIGURE 4. The U.S. version of the Reverser, called U-turn. (70-50-0495-1002pb01)

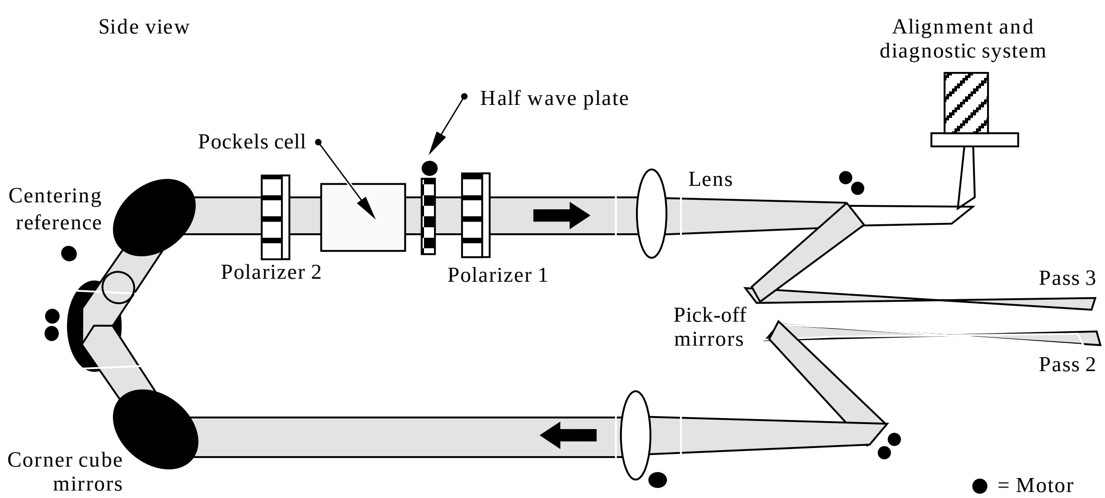

Since our primary goal was to prove viability of the Reverser concept, we did not modify the Beamlet layout for optimum Reverser performance. We added the Reverser hardware and removed the large Pockels cell and the harmonic generators, which were not needed. Figure 5 shows the baseline Beamlet layout, indicating the location of the Reverser hardware in the center of the transport spatial filter. All the Reverser components fit within the existing transport spacial filter's 24-in.-diam vacuum tube, and existing ports on the tube were used for access. Figure 6 shows the U-turn corner cube mounted in the mid-section of the Beamlet transport spatial filter.

Figure 3 illustrates the configuration of the L-turn that was tested on Beamlet. The beam enters through the pass 2 pinhole on the lower right, makes two passes through all the L-turn optics, and exits through the pass 3 pinhole. The alignment and diagnostic system includes a calorimeter for determining the energy of the pulsed beam, and a near-field camera that can image any of the components during alignment or at shot time. A motorized cavity mirror provides pointing adjustments during routine alignment. The half-wave plate was inserted during alignment to allow transmission of the system alignment laser. As shown, other components were also motorized to allow adjustment under vacuum, but they were only needed for the initial setup.

Figure 4 illustrates the U-turn layout, which we tested. It has similar optics to simplify conversion between the two layouts. Only the corner cube mirrors and the two pick-off mirrors replace corresponding components of the L-turn. The pass-2 lens was present for the L-turn, but not used. When reconfiguring from the L-turn, polarizer 2 had to be rotated 90° and the half-wave plate was inserted during shot time and removed for alignment.

For both L- and U-turn tests, the temporal and spatial profiles of the injected beam from the front end were the same as they had been for previous tests with the baseline configuration.[3] The injected beam had a parabolic spatial profile, higher at the edges than the center by about a factor of two, to compensate for gain roll-off toward the edges of the amplifiers. The input pulse was shaped temporally to compensate for gain saturation and to give an approximately square pulse

FIGURE 6. The middle section of the Beamlet transport spatial filter (end section removed). The corner-cube assembly of the U-turn is shown inside the 2-ft-diam tube. (70-50-0595-1191pb01)

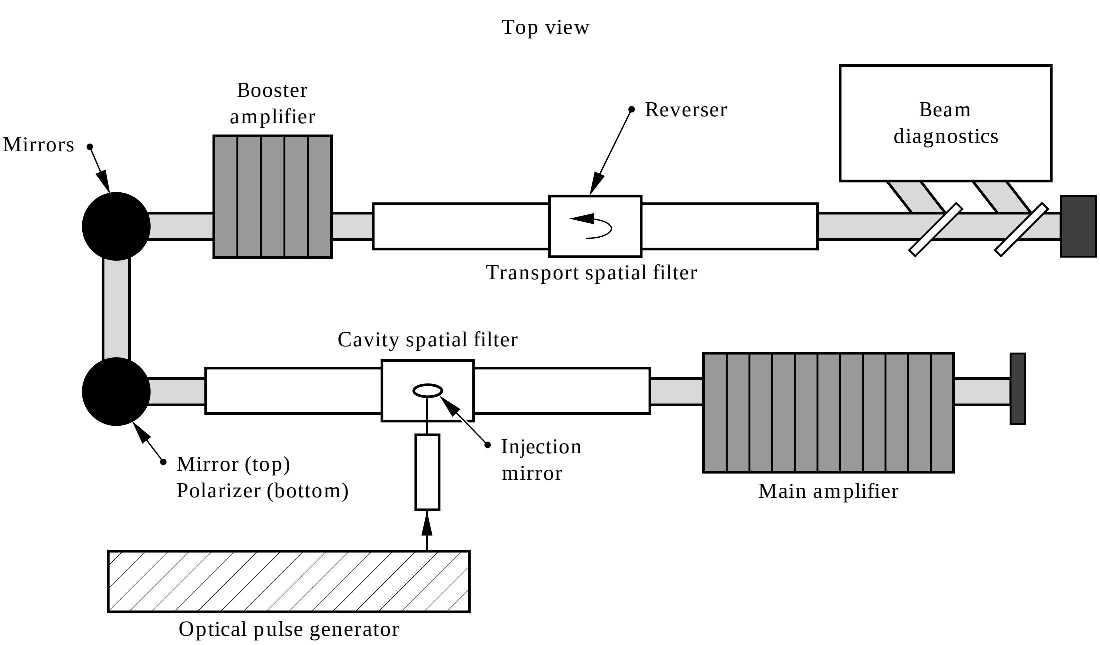

FIGURE 5. The Reverser's position in the transport spatial filter of the Beamlet laser. (70-50-0495-1001pb01)

at the output. The main beam was 32.5 cm square at its 10^{-2} intensity boundary with corners rounded at a radius of 5 cm and a fill factor of 84% (defined as the ratio of the beam energy to the energy if the entire 32.5×32.5 cm^2 beam were filled at the fluence of the central area of the beam).

The focal length of the lenses in the L- and U-turn optics was 110 cm to give a 4.0-cm square beam at the 10^{-2} intensity point in the collimated sections. The corresponding beam size on the first pick-off mirror was 2.2 cm square. For the L-turn, the angle between passes 2 and 3 was 27.3 mrad. The Pockels cell was a cylindrical-ring-electrode type with a 95% deuterated potassium dihydrogen phosphate (KD*P) crystal, an aperture of 7.3 cm in diam, and a length of 9.2 cm. The polarizers transmitted ≥97% of the *p*-polarized light and rejected up to 99.8% of the *s*-polarized light. The measured damage threshold of the polarizers was ≥10 J/cm^2 at 1.5 ns. In the L-turn configuration, the pulse length was limited to 2.3 ns to avoid beam overlap on polarizer 2.

L-Turn Tests

We arbitrarily chose to test the L-turn configuration first. In its original configuration, we used only polarizer 1 in the isolation unit. The Pockels cell was oriented such that it gave a quarter-wave retardation for a single pass with no applied voltage. The resulting isolation was 8×10^{-4}, good for a Pockels cell and polarizer of that aperture, but not enough to protect the front end against back reflections from lenses in the transport spatial filter. To increase the isolation, we added polarizer 2, as shown in Fig. 3, and oriented the Pockels cell for zero retardation with no applied voltage. Then, back-reflected energy made two complete passes through the isolation unit to reach the front end, and the isolation improved to 1.5×10^{-5}. This reduced the back-reflected energy at the front end to that of the injected energy, a level for which the front end was adequately isolated. The transmission through the L-turn was 53%.

Figure 7 shows the output fluences (energy per unit area) for the L-turn and baseline architectures as functions of input energy. Output fluence was used for the comparison rather than output energy, because the beam size for the L-turn was slightly smaller, 32.5 vs 34 cm square, to avoid clipping on the turning mirrors. (The turning mirror mounts were designed to clear only one pass, as required for the baseline. In the Reverser configuration, the beam reflects three times off the turning mirrors at offset positions. Since the mounts were not big enough to clear the three offset positions, we reduced the beam size slightly.) The maximum output energies for the L-turn at 2.3 ns and the baseline at 3 ns were 11.0 and 12.5 kJ, respectively. Note that the L-turn input energy required for a given output was 10 times less than for the baseline, because of the two extra passes through the booster amplifier. Clearly, the L-turn architecture gives comparable energy performance to the Beamlet baseline.

Figure 8 shows output irradiance (power per area) relative to output fluence (energy per area) for Beamlet. The Beamlet baseline architecture was originally optimized to provide maximum performance at 3 ns, but tests were also conducted at other pulse lengths, as shown. Outputs were limited by potential optical damage due to self-focusing at pulse lengths below 3 ns, and by the damage threshold of the polarizer above 3 ns. The shaded area in Fig. 8 indicates the maximum expected output at varying pulse lengths. The 11-kJ L-turn shot is the maximum irradiance attempted on Beamlet to date.

Because the large Pockels cell was removed for the Reverser tests, the amount of glass in the beamline was less, lowering the potential for nonlinear growth of output modulations. However, the two additional beam passes through the booster amplifier and the two

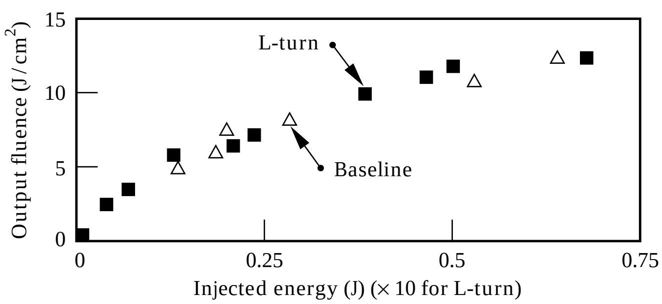

FIGURE 7. Injected energy vs output fluence for the Beamlet baseline and with the L-turn. The L-turn input energy required for a given output was 10 times less than for the baseline due to the two extra passes through the booster amplifier. (70-50-0495-1096pb01)

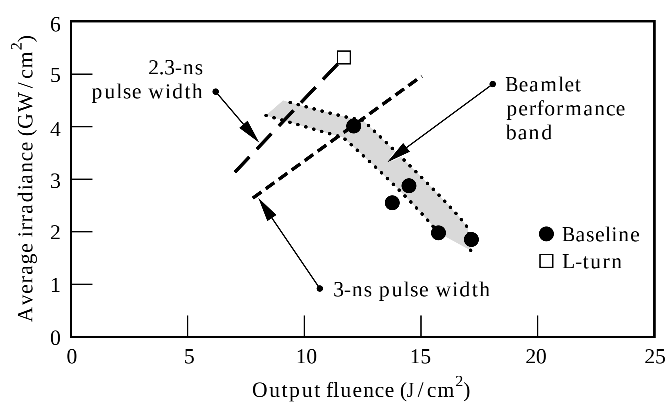

FIGURE 8. Irradiance vs fluence for Beamlet baseline and L-turn shots. (05-00-0494-2167pb01)

passes through the L-turn optics added aberrations. Consequently, the output modulation for the L-turn was slightly worse than for the baseline. For example, Fig. 9(a) shows the near-field image of the L-turn output at 4.3 GW / cm^2, which is equivalent to the highest irradiance baseline shot at 4.2 GW / cm^2. This image is a cumulative intensity distribution for the flat-top area of the output beam. There are 400×400 pixels, with each pixel corresponding to a beam area of 0.7×0.7 mm. Figure 9(b) shows horizontal and vertical lineouts. The peak-to-average fluence modulation in the image was 1.4:1. The comparable baseline modulation at this irradiance was 1.3:1.

Figure 10 shows near-field image data from L-turn shots at three values of peak irradiance. The number of pixels at each fluence (normalized to the maximum) is plotted vs that fluence (normalized to average fluence). There is virtually no difference between the modulation at 1.53 and 4.25 GW / cm^2. However, at 5.4 GW / cm^2, the modulation jumps from 1.4 to 1.5, implying the onset of nonlinear growth. To avoid risking optical damage, this regime of nonlinear growth is generally avoided, limiting the performance of the laser. This type of increase in modulation has also been observed in the baseline configuration.[3]

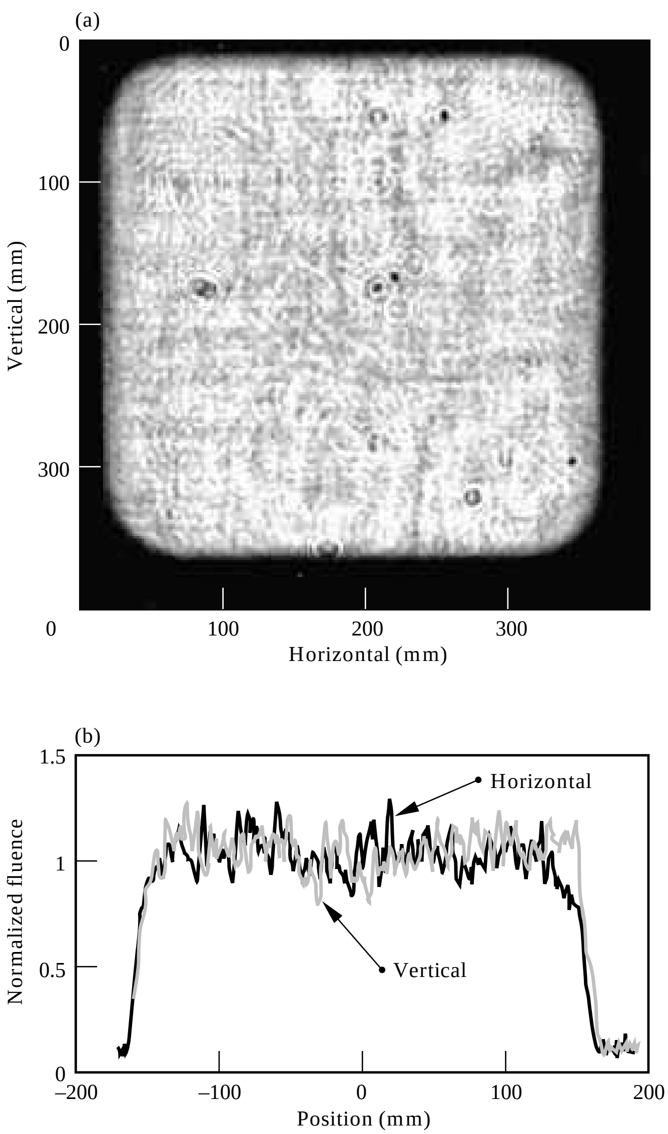

FIGURE 9. Near-field (a) image of the output beam with the L-turn at 4.3 GW / cm^2 and (b) horizontal and vertical lineouts through the image. (70-50-0595-1265pb01)

U-Turn Tests

In the U-turn configuration tests, the isolation provided by one pass through the polarizers and Pockels cell was 1×10^{-4} (see Fig. 4), which was barely acceptable for protection against back reflections. Note that the L-turn isolation was higher because the beam made two passes through the polarizer and Pockels cell. Conversely, the 70% U-turn transmission was better, because one pass through the isolation unit had less loss than the two passes with the L-turn.

Before the first U-turn tests, it was necessary to turn the L3 lens around so that the surface previously in vacuum was in air. Two damage spots on the vacuum side of L3 were created during tests before the L-turn experiments, and they increased to 6 and 8 mm at the lens surface during the L-turn shots. Since the vacuum side of the lens was in tension, these damage spots could have lead to crack propagation and lens failure, so the lens was turned around before the U-turn experiments began. This put the damage spots on the air

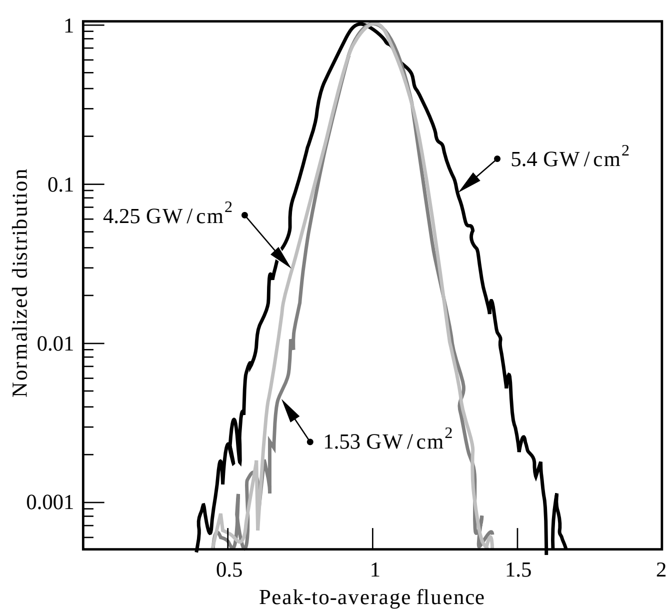

FIGURE 10. Near-field image data for output with the L-turn at three irradiances, showing nonlinear modulation growth at 5.3 GW / cm^2. (70-50-0595-1266pb01)

surface where they were in compression and not a threat to the lens integrity.

Attempting to duplicate the L-turn shots, the first U-turn shot delivered 780 J, but caused damage to several of the U-turn and front-end optics. In the front end, the injection mirror had a 1-mm portion of the coating removed, and small pits formed on the injection window and injection lens. In the U-turn, the pass 3 lens, both polarizers, and the Pockels cell had 1-mm damage, although none of the mirrors was damaged. In the Pockels cell, there were two damage tracks through the KD*P crystal.

The damaged components were replaced or repositioned, and low-energy shots allowed a detailed investigation of what caused the damage. Near-field images of the beam showed numerous pencil beams and ghost foci, but the most prominent was the one generated by L3's air surface. Reflectivity tests on the spatial filter lenses indicated that the antireflection coating (sol-gel) on that surface had deteriorated, from the typical value of about 0.1% to 3.2%. The measured reflectivities of the L3 vacuum surface and both L4 surfaces were normal. The cause of the coating deterioration is not known.

It became clear that turning the L3 lens around caused the U-turn to damage, whereas in L3's earlier orientation the L-turn was protected. This was because the deteriorated coating was on the vacuum-side during the L-turn tests. The vacuum side of the lens is concave with respect to pass 4, causing the reflection from that surface to focus in the air between the lens and booster amplifier. This focus causes the air to break down and absorb or deflect most of the energy in the reflection. Consequently, the unusually high energy of this reflection was greatly decreased by air breakdown, and the L-turn components were protected. However, when the lens was turned around at the start of U-turn tests, the defective coating went to the air surface of the lens, which is convex with respect to pass 4. The reflection from the convex surface did not focus, and consequently, there was no air breakdown to protect the U-turn optics.

We believe the optical damage was caused by parasitic pencil beams originating from the reflection off the air surface of L3. Figure 11 shows how the pass-4 output beam generates pencil beams from L3. (All beam passes through the lenses create reflections, but the final pass reflection is the most dangerous because it has the most energy.) Both reflections (one from each surface) pass through the booster amplifier and focus near the pinhole plane in the cavity spatial filter. Most of the light is blocked by the cavity pinhole plate, but some light passes through the pinholes forming three beams. (There are four pinholes, but the injection mirror blocks light from going through pinhole 1.) These beams are diffraction limited, and they remain small throughout the laser, from a couple of millimeters to about 1 cm, thus, the name "pencil beams." Because these pencil beams propagate parallel to the shot beam, they pass through the amplifiers and increase in fluence.

The pencil beam that caused damage in the U-turn was formed by cavity pinhole 4. That pencil beam continued backwards through the system to pass through the main amplifier twice, through cavity pinhole 3, through the booster amplifier, through pinhole 3 in the transport spatial filter, and into the U-turn. With a calculated fluence of around 270 J/cm^2, this pencil beam was more than sufficient to damage optics. Five factors contributed to this pencil beam's high fluence. (1) It had 15 to 30 times more energy than typical, because the coating reflected 3.2% rather than the typical 0.1 to 0.2%. (2) It propagated through both amplifiers twice, experiencing a gain of about 1200× before entering the Reverser. (3) It was down collimated into the Reverser (in this case 32.5- to 4-cm^2), which magnified the fluence of the pencil beam by a factor of 66. (4) It focused near the U-turn Pockels cell, which further increased its fluence by about 2×. (5) It was generated during a low-output-energy shot, 780 J, that was close to the most dangerous output with respect to back reflections. (As laser output energy is increased, gain saturation reduces the amount of energy left to amplify back reflections. Therefore, the highest-energy back reflections do not occur at maximum output but at about 2-kJ output.) Note that factors 1, 2, and 5 are system factors, and only factors 3 and 4 relate to the Reverser.

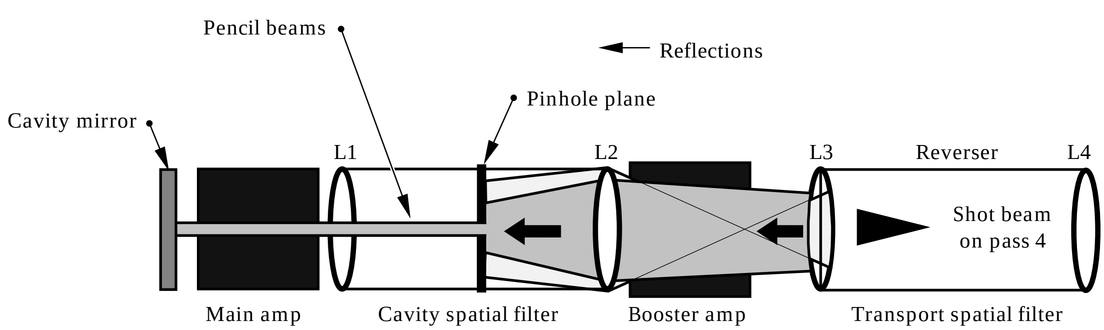

FIGURE 11. Reflections from the input lens to the transport spatial filter lens, L3, are formed into pencil beams by the pinholes in the cavity spatial filter. (70-50-0495-1004pb01)

Some energy from this same pencil beam passed through the U-turn as it damaged the Pockels cell and continued in reverse direction along passes 2 and 1. This energy was amplified by another pass through the booster amplifier and two more passes through the main amplifier, resulting in enough fluence to damage the injection mirror. The source of the damage to the injection lens and window was traced to a different pencil beam from the same L3 air surface. This pencil beam was formed by pinhole 2 in the cavity spatial filter, passed twice through the main amplifier (backwards along passes 2 and 1), and focused enough to damage the injection window and injection lens. It is important to emphasize that this damage had nothing to do with the U-turn and would have occurred in the baseline configuration if L3's air surface reflectivity had been 3%.

Two attempts were made to eliminate the L3 pencil beams—tilting L3 and inserting a beam block on the cavity mirror. Tilting L3 far enough eliminates the pencil beams by preventing its reflections from illuminating the pinholes in the cavity spatial filter. However, this required a tilt of more than 2°, which caused unacceptable output aberrations. The goal of the second scheme was to absorb the pencil beams with a 1-cm disk of absorbing glass fixed on the cavity mirror. The beams were blocked, but diffraction around the edges of the glass caused an unacceptable 20% increase in output beam modulation.

A more ambitious solution would have been to reduce the energy of the pencil beams at the Reverser by taking the Pockels cell and polarizer out of the Reverser and locating them at full-aperture near the cavity mirror, as shown in Fig. 12. In this configuration, the Pockels cell would cause half-wave retardation with applied voltage and zero retardation with no applied voltage. Unlike the NIF baseline, this Reverser architecture uses the Pockels cell and polarizer only for isolation and not to switch the beam from the cavity. Consequently, this isolation unit can be located anywhere in the beamline. By being located at the start of pass 4 (near the cavity mirror), the Pockels cell and polarizer reject the back reflections at full aperture and after only one pass through the amplifiers. This lowers the fluence of the pencil beams entering the Reverser by a factor of more than 10,000. This change would also be effective in eliminating other types of back reflections such as from pinholes or targets. It does, however, require a full-aperture Pockels cell and polarizer, which would eliminate some of the initial appeal for the Reverser concept, but the other benefits remain. This change is of interest for future Beamlet tests, but moving the large Pockels cell and polarizer would have taken longer than the remaining time available for these Reverser experiments. As a result, we did not risk damage by taking any more high energy shots.

Summary

These experiments demonstrated the basic viability of the Reverser concept. They showed that the concept of turning pass 2 into pass 3 with small mirrors and lenses in the transport spatial filter is valid. The Reverser output compares well with the results for the baseline architecture, and it achieved the highest irradiance output to date on Beamlet of 5.3 GW/cm^2. We encountered no problems with ASE or degradation to optics due to pinhole blowoff or vacuum conditions. Also, routine alignment of both L- and U-turn architectures was straightforward.

These experiments also exposed a serious weakness. They identified the inadequacy of a small-aperture isolation unit to protect the laser against back reflections. Although the damage to the front end from the L3 pencil beams would have occurred even with the baseline architecture, the severity of the damage to the Reverser optics resulted from two features of this Reverser design. (1) Back reflections make two complete passes through the amplifiers before entering the Reverser. (2) Back reflections are down collimated into the Reverser, magnifying their fluence by a large factor.

A change to the Reverser design would provide much greater tolerance to back reflections. Moving the isolation unit so that it attenuates the back reflections sooner along their backwards path through the laser substantially reduces their maximum fluence. With the Reverser, the Pockels cell and polarizer are not used to

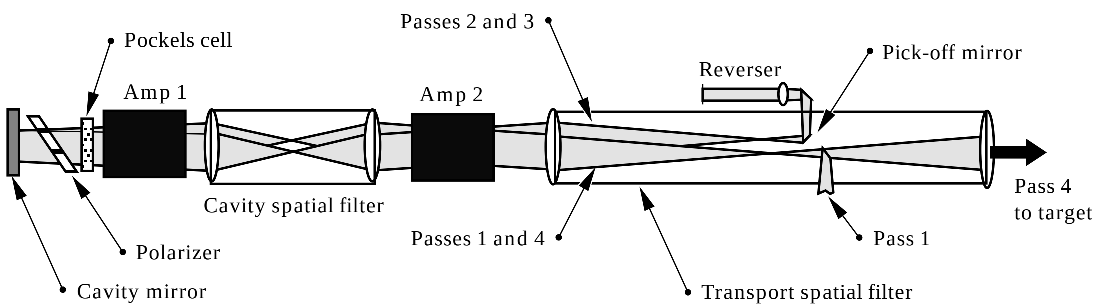

FIGURE 12. Locating a full-aperture Pockels cell near the cavity mirror would provide better isolation. (70-50-0595-1187pb01)

switch the beam from the cavity, so they can be located anywhere. One attractive location is near the start of pass 4, where the fluence of the out-going pulse is lower than in its baseline position, and where it attenuates reflections from final optics after only one backwards pass. This location for the isolation unit provides significantly better tolerance to back reflections. Therefore, we are considering a large Pockels cell and polarizer at this location for future Reverser tests on Beamlet.

Acknowledgments

The authors are grateful for the insight and direction provided by Howard Powell* and Michel Andre,† and for significant contributions from the technicians—Mireille Guenet,† Alain Pierre,† Cal Robb,* Dave Roberts,* Raymond Rossage,† and Ron Wing.* We also thank Mark Rhodes for managing the offline Pockels cell test.

Notes and References

1. *Avant Projet Sommaire*, Laser Megajoules, Direction Des Applications Militaires (CEA), 14 March, 1995.
2. J. Paisner, *National Ignition Facility Conceptual Design Report*, Lawrence Livermore National Laboratory, Livermore, CA, UCRL-PROP-117093 (May 1994).
3. B. M. Van Wonterghem, et al, *ICF Quarterly Report* 5(1), 1–17, Lawrence Livermore National Laboratory, Livermore, CA, UCRL-LR-105821-95-1 (1994).

*Lawrence Livermore National Laboratory, National Ignition Facility Project, Livermore, California
†Centre d'Études de Limeil–Valenton, Laser Megajoules, Valenton, France